Exp. Anim. 67(2), 291–299, 2018

—Original—

Quantitative angiographic anatomy of the renal arteries and adjacent aorta in the swine for preclinical studies of intravascular catheterization devices

Atsushi SAKAOKA[1,2)], Masafumi KOSHIMIZU[1)], Shintaro NAKAMURA[1)], and Kiyoshi MATSUMURA[2)]

[1)]*Evaluation Center, R&D Administration and Promotion Department, Terumo Corporation, 1500 Inokuchi, Nakai-machi, Ashigarakami-gun, Kanagawa 259-0151, Japan*
[2)]*Graduate School of Engineering, Osaka Institute of Technology, 5-16-1 Omiya, Asahi-ku, Osaka 535-8585, Japan*

Abstract: Swine are the most common animal model in preclinical studies of cardiovascular devices. Because of the recent trend for development of new devices for percutaneous catheterization, especially for the renal arteries (RAs), we examined the quantitative anatomical dimensions of the RAs and adjacent aorta in swine. Angiographic images were analyzed in 66 female Yorkshire/Landrace crossbred swine. The diameter of both the right and left main RA was 5.4 ± 0.6 mm. The length of the right main RA was significantly longer than that of the left (29.8 ± 7.5 mm vs. 20.6 ± 5.4 mm, respectively; $P<0.001$). The diameter of both the right and left branch RA with diameters ≥3 mm (the target vessel diameter of recently developed devices) was 3.8 ± 0.5 mm. The right branch RA was significantly longer than that of the left (18.9 ± 7.8 mm vs. 16.4 ± 7.4 mm, respectively; $P<0.05$). The branching angle of the right RA from the aorta was significantly smaller than that of the left (91 ± 12° vs. 103 ± 15°, respectively; $P<0.001$). The diameters of the suprarenal and infrarenal aorta were 10.6 ± 1.1 mm and 9.7 ± 0.9 mm, respectively. In conclusion, because of their similar dimensions to human, swine are an appropriate animal model for assessing the safety of, and determining optimal design of, catheter devices for RAs in simulated clinical use. However, there were species differences in the branching angle and adjacent aorta diameter, suggesting that swine models alone are inadequate to assess the delivery performance of catheter devices for RAs.

Key words: angiography, aorta, percutaneous catheterization, renal artery, swine

Introduction

Swine are the most common animal model used in preclinical studies of cardiovascular devices because of their physiological and anatomical similarities with humans [2, 9, 22, 28, 29]. In terms of development of cardiovascular devices, there is a recent trend for developing devices for percutaneous catheterization, which is a less invasive treatment than surgical operation, to minimize the burden on patients. The renal arteries (RAs) are one of the target vessels for percutaneous catheterization. Intravascular balloon catheters and stents have already been commercialized to dilate stenotic lesions in the RAs. Further, renal sympathetic denervation (RDN) has

(Received 9 October 2017 / Accepted 28 December 2017 / Published online in J-STAGE 19 January 2018)
Address corresponding: A. Sakaoka, 1500 Inokuchi, Nakai-machi, Ashigarakami-gun, Kanagawa 259-0151, Japan

emerged as a novel treatment option for hypertension to irreversibly suppress renal sympathetic activity using intra-RA catheters [1]. Although RDN devices have not yet been commercialized in Japan or the US, RDN devices adopting various technologies (e.g., heating with radiofrequency or ultrasound emission, and injection of neurotoxin with puncture needles) have been actively developed [4, 8, 24–26].

Despite common use of swine, there are only limited data on the anatomy of the porcine RAs. While a similar branching RA pattern was reported between swine and human [5, 21], no anatomical dimensions have been described. As the RAs are the direct anatomical target for catheter insertion, their dimensions can affect mechanical injury by direct contact of catheters, thermal injury, and mechano-chemical injury by puncture injection of a toxin. The RA dimension is also critical during *in vivo* testing of prototypes for design optimization (e.g., the radial force of an electrode on the arterial wall, and length or shape of the puncture needle). Moreover, in preclinical studies of cardiovascular devices, it is required by regulatory agencies and international standards to assess *in vivo* performance for safe delivery of intravascular catheters to the target structure and deployment of the device as intended [9, 13, 14]. The performance of insertion and deployment in RAs is affected by the RA dimension, the RA branching angle from the aorta, and the diameter of the adjacent aorta [33]. Therefore, it is important to understand the similarities of RA dimensions between swine and human to predict the safety and performance of RA devices in the clinical setting based on preclinical findings.

The aim of the present study was to investigate the quantitative anatomical characteristics of the RA in swine, including RA dimensions, branching angle of the RA from the aorta, and the diameter of the adjacent aorta, using catheter angiography, the gold standard in percutaneous catheterization, and to describe their similarities to human.

Materials and Methods

Animals

All procedures involving animals were approved by our Institutional Animal Care and Use Committees. A total of 66 female Yorkshire/Landrace crossbred swine (51.0–75.2 kg, 3.9–5.4 months old) were supplied from San-esu Breeding (Chiba, Japan) and Palmetto Research Swine (Reevesville, SC, USA). Females were selected as urethral catheterization for enhancement of urinary excretion of administered contrast media for angiography is only possible in females [30].

Experimental procedures

All animals were pre-medicated with aspirin (325 or 330 mg per os) from a minimum 1 day prior to the procedure. After anesthesia induction, swine were intubated and connected to mechanical ventilation. Anesthesia was maintained with 2–4% sevoflurane or 0.5–5% isoflurane by inhalation throughout the procedure. Anticoagulation during catheterization was achieved with intravenous heparin (100–300 units/kg) to maintain the activated clotting time at ≥250 s, as typically performed in clinical practice. A 6F or 7F introducer sheath was placed by percutaneous cannulation of the femoral artery, and a 6F or 7F guiding catheter was advanced to approach the RAs. Angiographic images of the aorta were acquired by administration of contrast media from the guiding catheter located in the aorta around the RAs. Intra-arterial nitroglycerin (200 μg) was then administered into the right and left RAs, followed by selective renal angiography by administration of contrast media from the guiding catheter into the right or left RAs. Angiographic images were acquired by C-arm angiography machines with Infinix Celeve-i INFX-8000V (Toshiba Medical Systems, Tochigi, Japan), GE Innova 3100 (GE Healthcare, Milwaukee, WI, USA), or Philips Allura Xper FD10 (Phillips Healthcare, Amsterdam, the Netherlands) flat detectors.

Measurement procedures

Angiographic images obtained prior to any treatment with test devices were retrospectively analyzed in the present study. The diameter of the RAs and their adjacent aorta, and the length of the RAs (Fig. 1 and Table 1), were measured with a CAAS 2000 (Pie Medical Imaging, Maastricht, The Netherlands)-based quantitative vascular analysis software using an automated edge detection system. The mean diameter was automatically calculated in the measured segment. A calibration process was performed prior to each measurement to determine the millimeter-to-pixel ratio of the angiographic images based on the size of the guide catheter in each image. The branching angle of the RAs from the aorta were measured with imaging software (ImageJ [27]; NIH, Bethesda, MD, USA). The diameter of the suprarenal

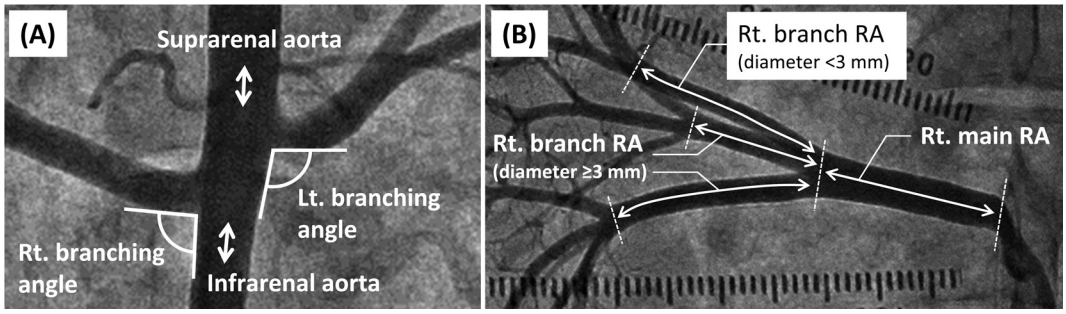

Fig. 1. Illustration of measured vasculatures in angiographic images. (A) The right and the left branching angles of renal arteries (RAs) from the aorta were measured. The diameters of the suprarenal and the infrarenal aorta were measured at the superior and inferior positions of the RAs, respectively. (B) The diameters and lengths of the RAs were measured. The main RA was defined as a single arterial segment from the renal ostium to the first bifurcation. The branch RAs were defined as all arterial segments at the post-bifurcation. Among the branch RAs, the segments that had a diameter ≥3 mm were measured. If the measured diameter was <3 mm, the values were excluded from data analysis. Rt., right; Lt., left.

Table 1. Measured vasculatures and selection rationale

Measured vasculature and parameter	Rationale of parameter selection
Diameter and length of main RA (right and left)	Applied segments of most current intravascular devices for RAs
Diameter and length of branch of RA with diameter ≥3 mm (right and left)	Applied segments of recently developed RDN devices[a)]
Branching angle of RA from the aorta (right and left)	Angles affecting deliverability of catheters into RA
Diameter of suprarenal and infrarenal aorta	Segments affecting deliverability of catheters into RA

[a)]The Symplicity Spyral (Medtronic, Minneapolis, MN, USA) and the IberisBloom (Terumo, Tokyo, Japan). RA=renal artery. RDN=renal sympathetic denervation.

aorta from one animal was not measured because of inadequate contrast of the acquired image.

Data analysis

Data are presented as mean ± SD. The following parameters between right and left main RA were compared with a paired *t* test: diameter, and length and branching angle from the aorta. The diameter and length between the right and left branch RA were compared with an unpaired t test. Pearson's correlation coefficients and scatter plots were used to investigate the correlation of body weight with dimensions of both the main RA and the branch RAs with a diameter ≥3 mm. All statistical analyses were performed with GraphPad Prism 7 (GraphPad Software, San Diego, CA, USA). A P-value<0.05 was considered to indicate statistical significance.

Results

The average diameter of the right and left main RAs was 5.4 ± 0.6 mm (Fig. 2A), with no differences between the right and left sides. The right main RA was significantly longer than that of the left main RA (29.8 ± 7.5 mm vs. 20.6 ± 5.4 mm, respectively; P<0.001) (Fig. 2B). The number of branch RAs with a diameter ≥3 mm was 1.6 ± 0.7 (range 0–3) for the right and left RAs. The average diameter of the right and left branch RA was 3.8 ± 0.5 mm, with no differences between the right and the left sides (Fig. 2A). The right branch RA was significantly longer than that of the left branch RA (18.9 ± 7.8 mm vs. 16.4 ± 7.4 mm, respectively; P<0.05) (Fig. 2B). There was no correlation of body weight with main RA dimensions (Fig. 3). In the branch RA, there were significant but weak positive correlations of body weight with all dimensions (r=0.22–0.27), except for the right branch RA length (Fig. 4).

The branching angle of the right RA from the aorta was significantly smaller than that of the left RA (91 ± 12° vs. 103 ± 15°, respectively; P<0.001) (Fig. 5). The diameters of the suprarenal and the infrarenal aorta were 10.6 ± 1.1 mm and 9.7 ± 0.9 mm, respectively (Fig. 6).

Discussion

The present study investigated the angiographic anatomical dimensions of the RAs and adjacent aorta in

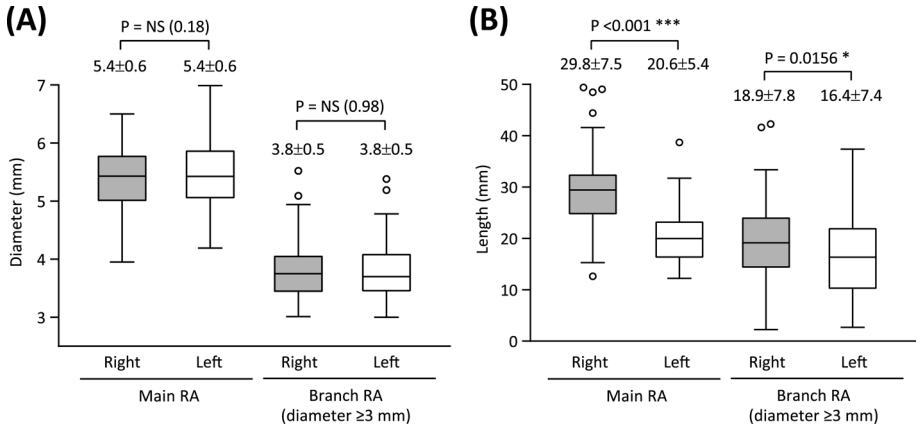

Fig. 2. Box plots of the diameter (A) and the length (B) of the RAs. Data are mean ± SD. *P*-values are shown in each plot.

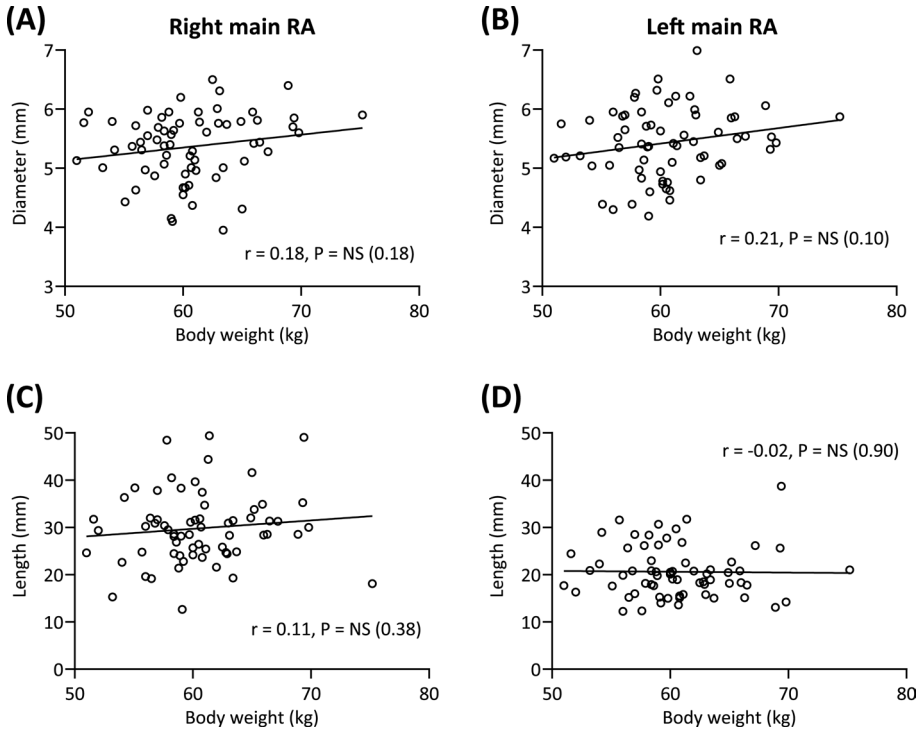

Fig. 3. Scatter plots between body weight and dimensions of the main RA. The dimension parameters included the diameters of the right (A) and left (B) main RAs, and the lengths of the right (C) and left (D) main RAs. Pearson's correlation coefficients (r) and *P*-values are shown in each plot.

Yorkshire/Landrace crossbred swine, which are commonly used for *in vivo* evaluation of cardiovascular devices. Despite the numerous preclinical studies of intra-renal-arterial catheter devices, these anatomical dimensions were previously unknown in the swine, although the anatomical dimensions of the RAs and adjacent aorta were reported in humans.

The mean diameter of the human main RA was reported as 5–6 mm, with no differences between the right and the left sides (Fig. 7A) [6, 20, 23, 31, 32]. In the present study, the mean diameter of the porcine main RA was 5.4 mm, with no difference between the right and the left sides, which was equivalent to human. The mean length of human main RA was 41.2–43.7 mm for the

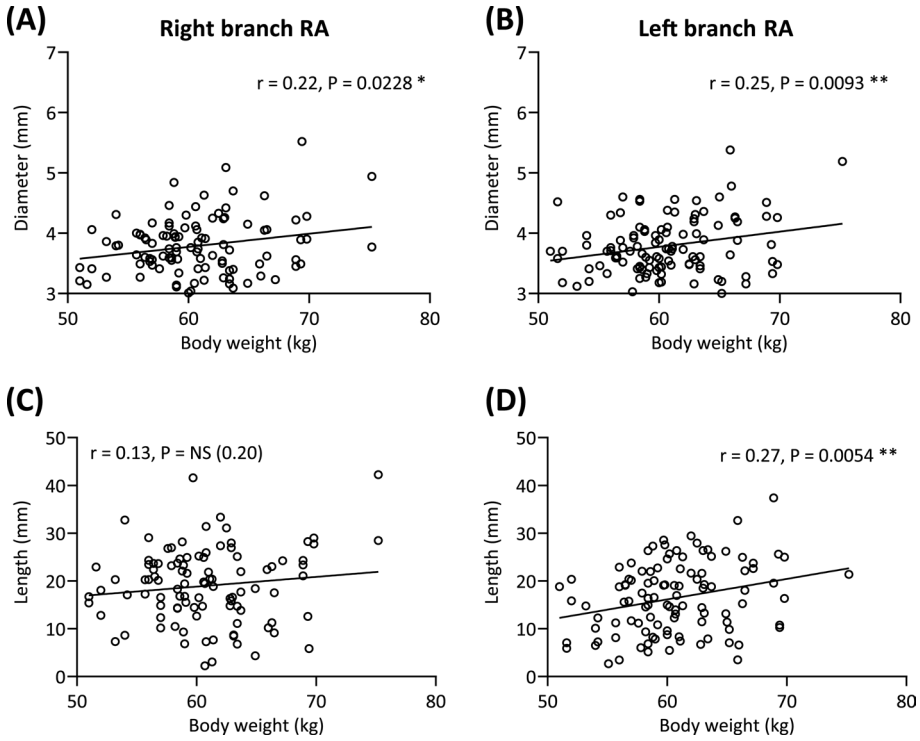

Fig. 4. Scatter plots between the body weight and the dimensions of the branch RAs with a diameter of ≥3 mm. The dimension parameters included the diameters of the right (A) and the left (B) branch RAs, and the lengths of the right (C) and the left (D) branch RAs. Pearson's correlation coefficients (r) and *P*-values are shown in each plot.

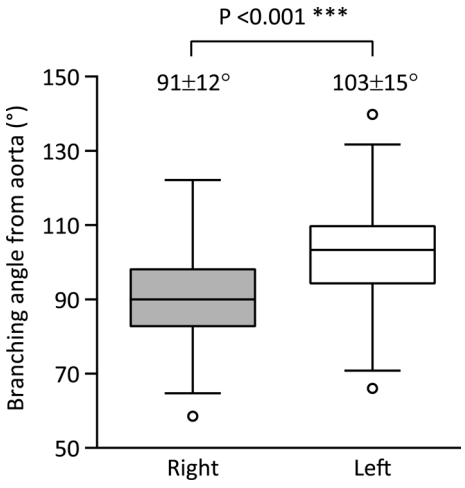

Fig. 5. Box plot of the branching angles from the aorta of the right and the left RAs. Data are mean ± SD. *P*-values are shown in each plot.

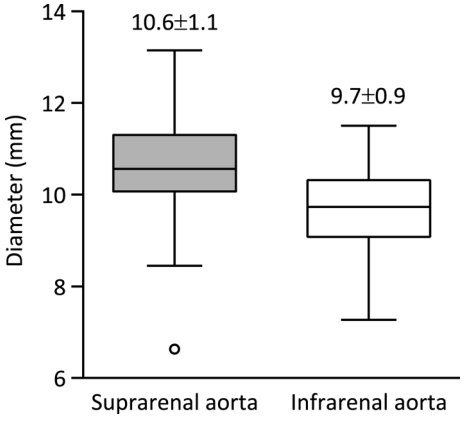

Fig. 6. Box plot of the diameters of the suprarenal and infrarenal aortas. Data are mean ± SD.

right RA and 32.2–36.5 mm for the left RA, which were significantly different by approximately 10 mm (Fig. 7B) [6, 20]. In the present study, the mean length of the porcine main RA was 29.8 mm for the right RA and 20.6 mm for the left RA, which was shorter than human RA by 11–16 mm. Nevertheless, as for the human, the right main RA was approximately 10 mm longer than the left RA in the swine.

The branching patterns of the RAs have been systematically investigated in swine and humans, including the number of arteries, distribution of branch arteries, sup-

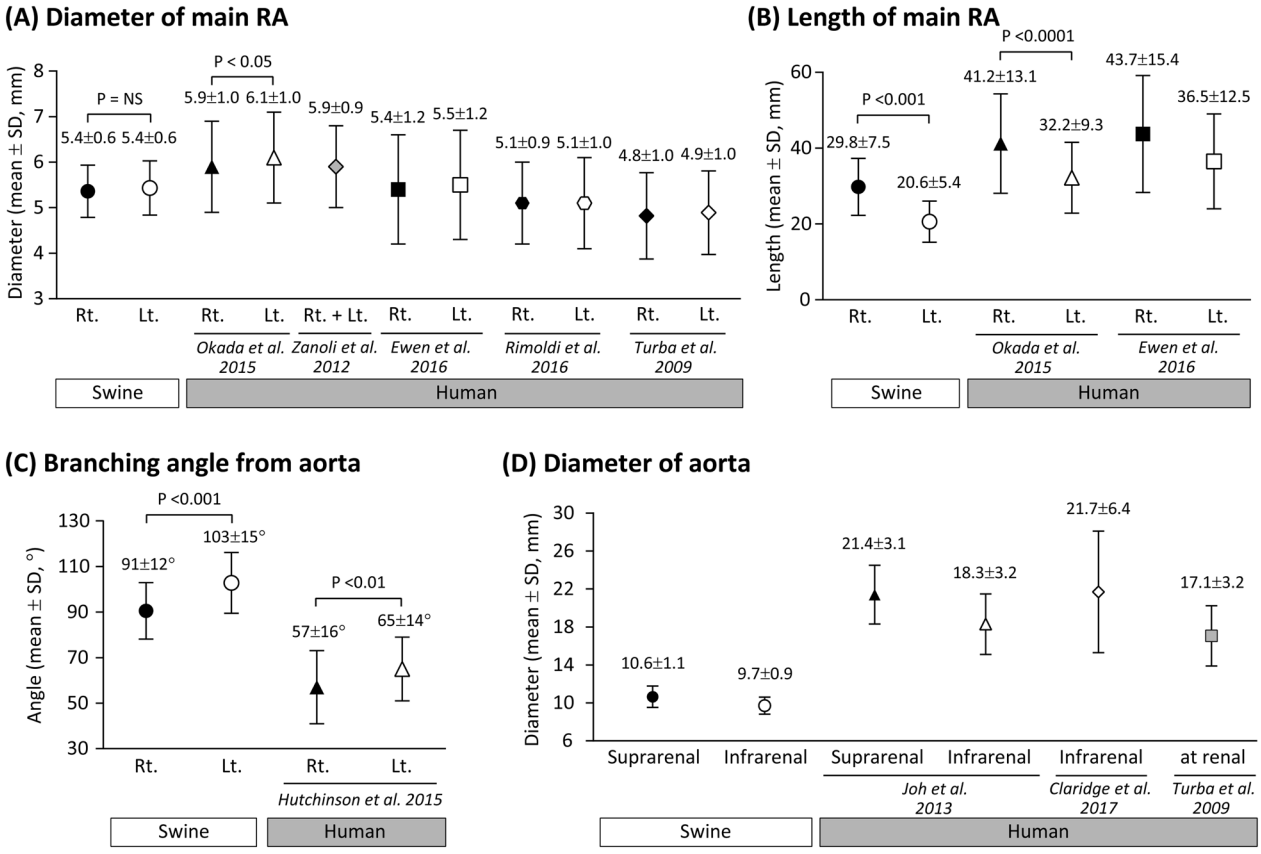

Fig. 7. Comparison of anatomical dimensions between swine and published human data. Each dot and error bar represent mean and SD, respectively. Data are mean ± SD. *P*-values are shown in each plot. (A) The diameter of the main RA. (B) The length of the main RA. (C) The branching angle of the RA from the aorta. (D) The diameters of the suprarenal and the infrarenal aortas.

plied renal zone of each branch artery, and their variability in terms of urological surgery, with many similarities between the two species [5, 21]. However, there are no studies examining the diameter or length of the branch RA in humans, likely because the main RA is the major clinical target for commercial balloons and stents to treat stenosis in RAs, and for most RDN devices under development. However, it was recently reported that an RDN targeting both the main and branch RAs had greater efficacy than an RDN in the main RA alone in animals [19] and humans [7]. Thus, interest in the anatomical dimensions of the branch RAs is expected to increase with further human studies. Considering the similarities of the branching patterns of the RAs between swine and humans, our data provide valuable information on the anatomical dimensions of branch RAs in the widely used preclinical swine model.

The mean branching angle of the RA from the aorta in human was acute in both the right RA (57°) and the left RA (65°) (Fig. 7C) [11]. While both swine and human show a right branching angle smaller than the left side (by approximately 10°), the right and left branching angles in swine were perpendicular or slightly obtuse, and larger than human branching angles by approximately 35°. In the current clinical standard procedure for percutaneous catheterization, a catheter is inserted from a femoral artery to access the RAs. In this situation, the catheter ascends the abdominal aorta from the punctured femoral artery, and then requires a large downward turn for insertion into the RAs. As such, insertion of a catheter into a RA in patients with a notable acute branching angle is technically difficult [10, 33]. Thus, as the porcine branching angle is less than that in humans, the delivery of catheter devices into the RAs will be easier in swine than in the clinical setting.

The mean diameter of the human aorta adjacent to the RAs was approximately 20 mm, approximately twice that of the porcine aorta (Fig. 7D) [3, 15, 31]. In gen-

eral, to deliver treatment catheters such as balloons, stents, and RDN devices to the target position, it is needed to stabilize a guiding catheter (a pathway for the treatment catheters) approaching the target vessel with adequate backup force. Less backup force is generated as the contact angle between the guiding catheter and the reverse side of the aorta decreases [12]. Further, the contact angle is generally lower when the catheter is located in a smaller diameter aorta. Thus, as the aortic diameter in swine was half of that in human, delivery of a guiding catheter into the RAs will be more difficult in swine than in the clinical setting.

A previous animal study reported moderate positive correlations of body weight with arterial diameter (r=0.35–0.62), and weak positive correlations of body weight with arterial length (r=−0.17–0.36), in porcine femoral and iliac arterial trees [17]. Based on these finding, we investigated the correlation of body weight with the anatomical dimensions of RAs in swine. However, we found no such correlations in the main RA, and only weak correlations in the branch RA, except for the right branch RA length.

Although healthy Yorkshire/Landrace crossbred swine are the most common animal model for *in vivo* studies using cardiovascular devices, healthy miniature swine are also used [22, 28]. Further, Ossabaw miniature swine fed with a high calorie diet were reported as a disease model of metabolic syndrome including hypertension [16], and the efficacy of an RDN device was assessed in the Ossabaw miniature swine [18]. Thus, assessment of the anatomical dimensions of the RAs in these swine models may also be useful in future studies.

The present study has several limitations. First, the catheter angiography images are theoretically projections of three-dimensional vessel structures onto a two-dimensional plane. Thus, the measured length may have been shorter than the actual length. Nevertheless, catheter angiography is the gold standard for morphological diagnosis during percutaneous catheterization in both preclinical studies and in the clinical setting, and is the most appropriate imaging modality for providing anatomical dimensions of RAs in preclinical studies. Catheter angiography was also used in the various clinical studies described above [6, 20]. Thus, our comparison of the length of the main RA between swine and human are based on the same imaging modality. Second, the anatomical dimensions in male swine were not investigated in the present study. However, we selected female swine as urethral catheterization to enhance urinary excretion of administered contrast media is only possible in females [30].

In conclusion, we determined the angiographic anatomical dimensions of RAs and adjacent aorta in swine. The length of the main RA was slightly shorter in swine than that in human, while the RA diameter and the right and left RA differences were similar between swine and human. Thus, swine are an appropriate animal model to assess the safety of, and to determine optimal design of, catheter devices for RAs in simulated clinical use. However, the branching angle of the RAs from the aorta was larger in swine than that in human, while the diameter of the adjacent aorta in swine was half of that in human. Thus, the swine model alone is inadequate to assess delivery performance of catheter devices for RAs.

Conflict of Interest

This study was supported by Terumo Corporation, Tokyo, Japan. The authors declare that there is no conflict of interest.

Acknowledgments

We thank Brad Hubbard, DVM, from Gateway Medical Innovation Center, Shanghai, China, and Edanz Group, for editing a draft of this manuscript.

References

1. Bertog, S.C., Sobotka, P.A., and Sievert, H. 2012. Renal denervation for hypertension. *JACC Cardiovasc. Interv.* 5: 249–258. [Medline] [CrossRef]
2. Byrne, R.A., Serruys, P.W., Baumbach, A., Escaned, J., Fajadet, J., James, S., Joner, M., Oktay, S., Jüni, P., Kastrati, A., Sianos, G., Stefanini, G.G., Wijns, W., and Windecker, S. 2015. Report of a European Society of Cardiology-European Association of Percutaneous Cardiovascular Interventions task force on the evaluation of coronary stents in Europe: executive summary. *Eur. Heart J.* 36: 2608–2620. [Medline] [CrossRef]
3. Claridge, R., Arnold, S., Morrison, N., and van Rij, A.M. 2017. Measuring abdominal aortic diameters in routine abdominal computed tomography scans and implications for abdominal aortic aneurysm screening. *J. Vasc. Surg.* 65: 1637–1642. [Medline] [CrossRef]
4. Daemen, J. 2013. Current technologies: an introduction. *EuroIntervention* 9:(Suppl R): R75–R82. [Medline] [CrossRef]
5. Evan, A.P., Connors, B.A., Lingeman, J.E., Blomgren, P., and Willis, L.R. 1996. Branching patterns of the renal artery

of the pig. *Anat. Rec.* 246: 217–223. [Medline] [CrossRef]
6. Ewen, S., Ukena, C., Lüscher, T.F., Bergmann, M., Blankestijn, P.J., Blessing, E., Cremers, B., Dörr, O., Hering, D., Kaiser, L., Nef, H., Noory, E., Schlaich, M., Sharif, F., Sudano, I., Vogel, B., Voskuil, M., Zeller, T., Tzafriri, A.R., Edelman, E.R., Lauder, L., Scheller, B., Böhm, M., and Mahfoud, F. 2016. Anatomical and procedural determinants of catheter-based renal denervation. *Cardiovasc. Revasc. Med.* 17: 474–479. [Medline] [CrossRef]
7. Fengler, K., Ewen, S., Höllriegel, R., Rommel, K.P., Kulenthiran, S., Lauder, L., Cremers, B., Schuler, G., Linke, A., Böhm, M., Mahfoud, F., and Lurz, P. 2017. Blood Pressure Response to Main Renal Artery and Combined Main Renal Artery Plus Branch Renal Denervation in Patients With Resistant Hypertension. *J. Am. Heart Assoc.* 6: e006196. [Medline] [CrossRef]
8. Fischell, T.A., Fischell, D.R., Ghazarossian, V.E., Vega, F., and Ebner, A. 2015. Next generation renal denervation: chemical "perivascular" renal denervation with alcohol using a novel drug infusion catheter. *Cardiovasc. Revasc. Med.* 16: 221–227. [Medline] [CrossRef]
9. Food and Drug Administration. 2010. Guidance for Industry and FDA Staff: General Considerations for Animal Studies for Cardiovascular Devices. https://www.fda.gov/MedicalDevices/ucm220760.htm
10. Goswami, N.J. and Goldstein, J.A. 2015. pp. 643–653. Renal Artery Stenosis. *In:* Textbook of Interventional Cardiology. (Topol, E., and Teirstein, P. eds.), Elsevier.
11. Hutchinson, B.D., Keane, D., and Dodd, J.D. 2013. Renal sympathetic denervation: MDCT evaluation of the renal arteries. *AJR Am. J. Roentgenol.* 201: W342–W346. [Medline] [CrossRef]
12. Ikari, Y., Nagaoka, M., Kim, J.Y., Morino, Y., and Tanabe, T. 2005. The physics of guiding catheters for the left coronary artery in transfemoral and transradial interventions. *J. Invasive Cardiol.* 17: 636–641. [Medline]
13. International Organization for Standardization. 2012. ISO 25539-2 Cardiovascular implants − Endovascular devices − Part 2: Vascular stents.
14. International Organization for Standardization. 2017. ISO 25539-1 Cardiovascular implants − Endovascular devices − Part 1: Endovascular prostheses.
15. Joh, J.H., Ahn, H.J., and Park, H.C. 2013. Reference diameters of the abdominal aorta and iliac arteries in the Korean population. *Yonsei Med. J.* 54: 48–54. [Medline] [CrossRef]
16. Kreutz, R.P., Alloosh, M., Mansour, K., Neeb, Z., Kreutz, Y., Flockhart, D.A., and Sturek, M. 2011. Morbid obesity and metabolic syndrome in Ossabaw miniature swine are associated with increased platelet reactivity. *Diabetes Metab. Syndr. Obes.* 4: 99–105. [Medline] [CrossRef]
17. Lopes-Berkas, V.C. and Jorgenson, M.A. 2011. Measurement of peripheral arterial vasculature in domestic Yorkshire swine by using quantitative vascular angiography. *J. Am. Assoc. Lab. Anim. Sci.* 50: 628–634. [Medline]
18. Mahfoud, F., Moon, L.B., Pipenhagen, C.A., Jensen, J.A., Pathak, A., Papademetriou, V., Ewen, S., Linz, D., and Böhm, M. 2016. Catheter-based radio-frequency renal nerve denervation lowers blood pressure in obese hypertensive swine model. *J. Hypertens.* 34: 1854–1862. [Medline] [CrossRef]
19. Mahfoud, F., Tunev, S., Ewen, S., Cremers, B., Ruwart, J., Schulz-Jander, D., Linz, D., Davies, J., Kandzari, D.E., Whitbourn, R., Böhm, M., and Melder, R.J. 2015. Impact of Lesion Placement on Efficacy and Safety of Catheter-Based Radiofrequency Renal Denervation. *J. Am. Coll. Cardiol.* 66: 1766–1775. [Medline] [CrossRef]
20. Okada, T., Pellerin, O., Savard, S., Curis, E., Monge, M., Frank, M., Bobrie, G., Yamaguchi, M., Sugimoto, K., Plouin, P.F., Azizi, M., and Sapoval, M. 2015. Eligibility for renal denervation: anatomical classification and results in essential resistant hypertension. *Cardiovasc. Intervent. Radiol.* 38: 79–87. [Medline] [CrossRef]
21. Pereira-Sampaio, M.A., Favorito, L.A., and Sampaio, F.J. 2004. Pig kidney: anatomical relationships between the intrarenal arteries and the kidney collecting system. Applied study for urological research and surgical training. *J. Urol.* 172: 2077–2081. [Medline] [CrossRef]
22. Perkins, L.E. 2010. Preclinical models of restenosis and their application in the evaluation of drug-eluting stent systems. *Vet. Pathol.* 47: 58–76. [Medline] [CrossRef]
23. Rimoldi, S.F., Scheidegger, N., Scherrer, U., Farese, S., Rexhaj, E., Moschovitis, A., Windecker, S., Meier, B., and Allemann, Y. 2014. Anatomical eligibility of the renal vasculature for catheter-based renal denervation in hypertensive patients. *JACC Cardiovasc. Interv.* 7: 187–192. [Medline] [CrossRef]
24. Sakakura, K., Roth, A., Ladich, E., Shen, K., Coleman, L., Joner, M., and Virmani, R. 2015. Controlled circumferential renal sympathetic denervation with preservation of the renal arterial wall using intraluminal ultrasound: a next-generation approach for treating sympathetic overactivity. *EuroIntervention* 10: 1230–1238. [Medline] [CrossRef]
25. Sakakura, K., Tunev, S., Yahagi, K., O'Brien, A.J., Ladich, E., Kolodgie, F.D., Melder, R.J., Joner, M., and Virmani, R. 2015. Comparison of histopathologic analysis following renal sympathetic denervation over multiple time points. *Circ. Cardiovasc. Interv.* 8: e001813. [Medline] [CrossRef]
26. Sakaoka, A., Takami, A., Onimura, Y., Hagiwara, H., Terao, H., Kumagai, F., and Matsumura, K. 2017. Acute changes in histopathology and intravascular imaging after catheter-based renal denervation in a porcine model. *Catheter. Cardiovasc. Interv.* 90: 631–638. [Medline] [CrossRef]
27. Schneider, C.A., Rasband, W.S., and Eliceiri, K.W. 2012. NIH Image to ImageJ: 25 years of image analysis. *Nat. Methods* 9: 671–675. [Medline] [CrossRef]
28. Schomberg, D.T., Tellez, A., Meudt, J.J., Brady, D.A., Dillon, K.N., Arowolo, F.K., Wicks, J., Rousselle, S.D., and Shanmuganayagam, D. 2016. Miniature Swine for Preclinical Modeling of Complexities of Human Disease for Translational Scientific Discovery and Accelerated Development of Therapies and Medical Devices. *Toxicol. Pathol.* 44: 299–314. [Medline] [CrossRef]
29. Suzuki, Y., Yeung, A.C., and Ikeno, F. 2009. The pre-clinical animal model in the translational research of interventional cardiology. *JACC Cardiovasc. Interv.* 2: 373–383. [Medline] [CrossRef]
30. Swindle, M.M. 2015. Urinary System and Adrenal Glands.

In: Swine in the Laboratory: Surgery, Anesthesia, Imaging, and Experimental Techniques. (Swindle, M.M., and Smith, A.C. eds.), CRC Press.

31. Turba, U.C., Uflacker, R., Bozlar, U., and Hagspiel, K.D. 2009. Normal renal arterial anatomy assessed by multidetector CT angiography: are there differences between men and women? *Clin. Anat.* 22: 236–242. [Medline] [CrossRef]
32. Zanoli, L., Rastelli, S., Marcantoni, C., Tamburino, C., Laurent, S., Boutouyrie, P., and Castellino, P. 2012. Renal artery diameter, renal function and resistant hypertension in patients with low-to-moderate renal artery stenosis. *J. Hypertens.* 30: 600–607. [Medline] [CrossRef]
33. Zeller, T. 2013. pp. 907–923. Endovascular treatment of renal arteries. *In:* Catheter-based cardiovascular interventions: A knowledge-based approach. (Lanzer, P. ed.), Springer-Verlag Berlin Heidelberg.